Applied Surface Science 318 (2014) 256–261

Contents lists available at ScienceDirect

Applied Surface Science

journal homepage: www.elsevier.com/locate/apsusc

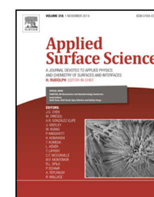

Spectroscopic ellipsometry study of Si nanocrystals embedded in a SiO_x matrix: Modeling and optical characterization

Serim Ilday [a,b,*], Gizem Nogay [b,c], Rasit Turan [a,b,c]

[a] Graduate Program of Micro and Nanotechnology, Middle East Technical University, Ankara, Turkey
[b] Center for Solar Energy Research and Application (GÜNAM), Middle East Technical University, Ankara, Turkey
[c] Department of Physics, Middle East Technical University, Ankara, Turkey

ARTICLE INFO

Article history:
Received 31 October 2013
Received in revised form 21 April 2014
Accepted 21 April 2014
Available online 28 April 2014

Keywords:
Spectroscopic ellipsometry
Silicon nanocrystal
SiO_x
Optical properties
Modeling
Magnetron-sputtering

ABSTRACT

In this work, we report on a spectroscopic ellipsometry study of thin films of silicon nanocrystals embedded in a SiO_x matrix that is performed to better understand how substoichiometric SiO_x species affect the optical properties of these systems. The silicon nanocrystals are fabricated in a SiO_x matrix by thermal annealing of magnetron-sputtered thin films in a wide range of x values ($0 < x < 2$) in order to produce every possible substoichiometric SiO_x species in various fractions. A generic optical model to describe the thin film content with various SiO_x volumetric fractions is developed and used to analyze the data obtained from the spectroscopic ellipsometry. Tauc-Lorentz and Bruggeman effective medium approximation models are employed to determine the ellipsometric angles (Ψ and Δ) and the complex dielectric function. We show that the optical properties of the nc-Si embedded in a SiO_x matrix are highly dependent on the value of x and on the volumetric fractions of the substoichiometric SiO_x species present in the system.

© 2014 Elsevier B.V. All rights reserved.

1. Introduction

Silicon nanocrystals (nc-Si) embedded in a dielectric matrix, most notably in SiO_x ($0 < x < 2$), constitute a promising thin-film material system for various optoelectronic devices, especially for photovoltaics [1]. Therefore, methods that allow identification of their optical and electronic properties efficiently are essential. Spectroscopic ellipsometry (SE) is a powerful, easy-to-use, and non-destructive tool that can be used to evaluate a wide range of thin-film properties such as film thickness, crystallinity, average nanocrystal size, chemical composition, surface roughness, optical and dielectric constants, and optical bandgap [2]. Due to its practicality, SE is often preferred over alternative optical characterization methods, especially for nanoscale semiconductor materials, including thin films of nc-Si embedded in a SiO_x matrix (nc-Si/SiO_x). However, the optical and electrical properties of these systems are strongly dependent on a wide range of parameters such as nanoscale material structure and type and chemical composition of the dielectric matrix. Moreover, these properties depend on the fabrication procedure, which makes it essential to identify the optical properties of these thin films. For these reasons, it is desirable to develop a generic optical model for SE studies that describes the system and characterizes the effect of these parameters. To date, SE studies on the nc-Si/SiO_x have been performed on thin films of SiO or SiO_2 on c-Si substrates [3–5], porous Si [6,7] and silicon-rich oxide/SiO_2 superlattices [6,8,9] and Si^+ implantation in SiO_2 [10]. However, none of these studies investigate the nc-Si/SiO_x, much less over a wide range of stoichiometries ($0 < x < 2$), including all possible substoichiometric SiO_x species in their analyses.

Here, we report on a SE study of nc-Si/SiO_x that is performed to better understand how substoichiometric SiO_x species affect the optical properties of these systems. The nc-Si are fabricated in a SiO_x matrix by thermal annealing of magnetron-sputtered thin films over a wide range of x values ($0 < x < 2$) in order to produce practically all possible substoichiometric SiO_x species in various fractions. We present a generic optical model to analyze the data obtained from SE and to characterize the thin film content with various SiO_x volumetric fractions. Validity of our model is verified through comprehensive X-ray photoelectron spectroscopy (XPS) and transmission electron microscopy (TEM) analyses over a wide range of x values. We further show that the optical properties of nc-Si/SiO_x systems depend strongly on their x-value and the volumetric fractions of the substoichiometric SiO_x species in the system.

* Corresponding author at: ODTU Fizik Bol. Z41, 06800 Cankaya, Ankara, Turkey. Tel.: +90 312 210 4324.
E-mail address: serim.ilday@metu.edu.tr (S. Ilday).

http://dx.doi.org/10.1016/j.apsusc.2014.04.153
0169-4332/© 2014 Elsevier B.V. All rights reserved.

2. Materials and methods

The nc-Si are fabricated inside a SiO_x matrix by thermal annealing of magnetron-sputtered thin films in a wide range of x values ($0 < x < 2$) in order to produce practically all possible sub-stoichiometric SiO_x species in various fractions. Approximately 300 nm-thick single layers of thin films are co-sputtered from 99.9% pure, 3″-diameter Si and SiO_2 targets onto p-type (1 0 0) oriented Si and quartz substrates. Depositions are performed at room temperature and 99.99% pure Ar is used as the process gas. In order to control the SiO_x composition ($0 < x < 2$) the DC power applied to the Si target is adjusted between $15\,W < P_{Si} < 150\,W$, while the RF power applied to the SiO_2 target is kept constant at 180 W. Post-annealing is done for 1 h under constant flow of N_2 at 1100 °C to promote nc-Si growth. Crystalline structure of the prepared films is verified through Raman spectroscopy (RS) (Horiba-Jobin Yvon i550), high-resolution transmission electron microscopy (HRTEM) (Jem Jeol 2100F 200 kV) and energy-filtered TEM (EFTEM) analyses (FEI Titan 80-300 microscope operating at an accelerating voltage of 300 kV and equipped with a Gatan Imaging Filter 863). Stoichiometry of the system and the volumetric fractions of the substoichiometric species are verified through X-ray photoelectron spectroscopy (XPS) analysis (PHI 5000 VersaProbe equipment with monochromatic Al K_α excitation as X-ray source). Ar^+ ion bombardment is used for XPS depth profiling studies, where Peakfit software (version 4.12) is used to fit the spectra. Thin film thicknesses are confirmed to be ∼300 nm through HRTEM and profilometer analyses. SE studies are performed using SEMILAB SOPRA GES5E equipped with Sopra Winelli II software. Ellipsometric angles, Ψ and Δ, are measured over the spectral range of 240–840 nm at 70° angle of incidence at room temperature with a xenon lamp as source. A generic optical model is developed to ascertain the thin film content of nc-Si/SiO_x based on the x values. The SiO_x volumetric fractions are extracted from XPS analyses. SE data is interpreted through Tauc-Lorentz (TL) and Bruggeman effective medium approximation (EMA) models. TL is used for parameterization of optical functions for a-Si and insulator matrix, whereas a combination of TL and EMA is used for the parameterization of the optical functions for the thin film structure that has multiple components (nc-Si, a-Si, SiO_x, SiO_2, and void).

3. Results and discussion

In order to develop a generic optical model for a complex system such as nc-Si/SiO_x, which consists of multiple components, it is important to first identify the chemical and structural properties of this system such as stoichiometry, thin film homogeneity, crystallinity, volumetric fractions and the chemical environment of the thin film components. The procedure is described step by step below.

First of all, the stoichiometry, x, of the SiO_x is identified from XPS analyses (Fig. 1). Fig. 1 shows a graph of variations in x with respect to the DC power applied to Si target material during magnetron sputtering. As can be seen from the figure, the stoichiometry varies over a wide range.

Next, the nanoscale Si crystallization within the thin films is verified through HRTEM imaging (Fig. 2) and RS (data not shown here) analyses. As can be seen from the figure that the nc-Si structures with an average diameter of 4 nm are formed in the dielectric matrix. In addition to that, we observe relatively small amounts of amorphous Si (a-Si) during RS analyses.

The homogenous structure of the thin films are confirmed through XPS depth profiling analyses performed on Si 2p signal as shown in Fig. 3, where first layer is the naturally grown surface oxide layer. The next four layers are layers of nc-Si/SiO_x that have both Si—O and Si—Si bonds distributed homogenously throughout the thin film. In the preceding layers there is the signal only for Si—Si bonds arising from the c-Si substrate.

XPS peak-fitting analyses are also performed on the Si 2p signal obtained from the post-annealed thin films in order to identify the chemical environment of the system, especially to ascertain

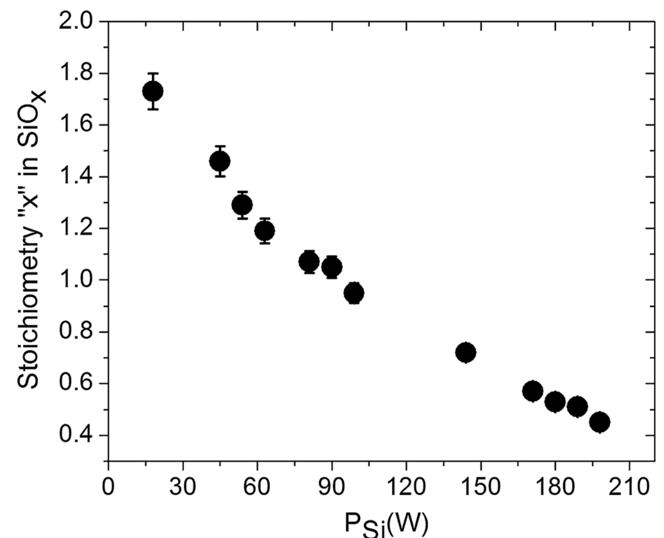

Fig. 1. Graph showing variations in stoichiometry with respect to the DC power applied to Si target material during magnetron sputtering.

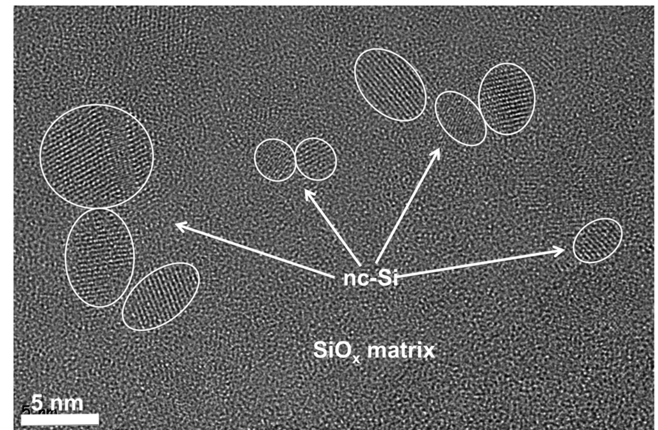

Fig. 2. HRTEM image showing nanoscale crystallization in the nc-Si/SiO_x with x = 1.3.

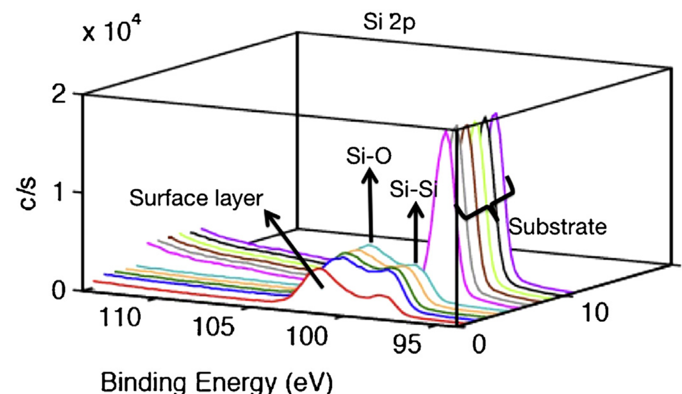

Fig. 3. Graph showing the XPS depth-profiling analyses performed on Si 2p signal of the nc-Si/SiO_x with x = 1.1.

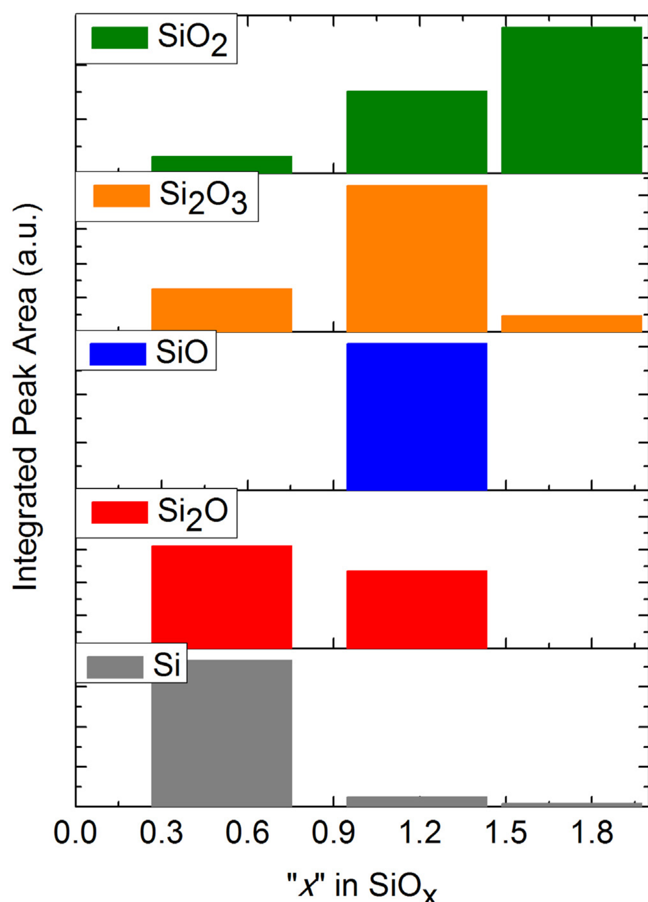

Fig. 4. Graph showing relative contributions of XPS signals emanating from substoichiometric (Si_2O, SiO, and Si_2O_3) and stoichiometric (Si and SiO_2) components to the Si 2*p* XPS spectra.

the type and volumetric fraction of the substoichiometric species (Si_2O, SiO, Si_2O_3) along with the stoichiometric Si and SiO_2 species (Fig. 4). Fig. 4 shows a graph of relative contributions of XPS signals emanating from the substoichiometric (Si_2O, SiO, and Si_2O_3) and stoichiometric (Si and SiO_2) components.

As can be seen from the figure, when x approaches 2 ($x > 1.3$), the system becomes SiO_2 rich. On the other hand, when x approaches 0 ($x < 0.9$), the system becomes Si rich. However, in the intermediate region ($0.9 < x < 1.3$) all substoichiometric SiO_x species can be observed along with the stoichiometric Si and SiO_2 species. Eventually, the nc-Si/SiO_x with various stoichiometries can be considered to have three representative regions: Si-rich ($x < 0.9$), SiO_2-rich ($x > 1.3$), and the intermediate ($0.9 < x < 1.3$) region, which mostly consists of substoichiometric SiO_x species.

In light of these analyses, we present a generic optical model to describe the content of the nc-Si/SiO_x with various SiO_x volumetric fractions (Fig. 5(a)). In this model, the thin film layer is described as a mixture of a-Si, nc-Si, SiO_x, SiO_2, and void as confirmed by XPS, RS, and TEM analyses.

The optical model shown in Fig. 5(a) provides excellent agreement with data obtained from the Si-rich region, whereas in order to successfully describe the intermediate and SiO_2-rich regions we have to ignore the interface layer by setting its thickness to 0. This can be explained by the nature and distribution of the substoichiometric species in the nc-Si/SiO_x: As in the case of intermediate and SiO_2-rich regions, Si—O bonds from SiO_x and SiO_2 species dominate the chemical environment of the thin film. Although there is an interface layer that is rich in Si—O bonds for these regions, the chemical environment of this interface is so similar to that of the

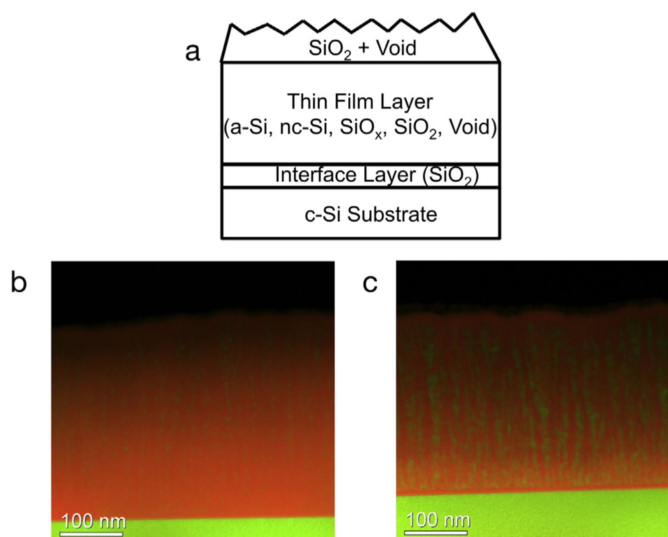

Fig. 5. (a) Schematic of the optical model developed to describe the content of the nc-Si/SiO_x with various SiO_x volumetric fractions for SE calculations. Superposition of the Si (green) and the SiO_x (red) plasmon EFTEM images obtained from nc-Si/SiO_x showing (b) no significant interface layer between the substrate and the thin film layer for the intermediate and SiO_2-rich regions, (c) a well-defined thin interface layer between the substrate and the thin film layer for the Si-rich region. (For interpretation of the references to color in this figure legend, the reader is referred to the web version of the article.)

thin film layer that it behaves as if the interface and the thin film layer are fused together (Fig. 5(b)). Consequently, there is no need to introduce an extra interface layer to the optical model. On the other hand, in the Si-rich region, nc-Si formation is much more prominent. Unlike the intermediate and SiO_2-rich regions, Si—Si bonds, surrounded by Si—O bonds, have a dominant influence on the thin film's chemical environment. This naturally evolves into a structure where a distinct SiO_2 interface layer forms between the film and the substrate [11,12]. The presence of the interface layer (red) between the c-Si substrate (green) and the thin film for the Si-rich region is established from EFTEM images (Fig. 5(c)).

The optical model shown in Fig. 5(a) is used in the mathematical fittings and calculations of the SE data obtained from the nc-Si/SiO_x and their optical properties are extracted from these fittings accordingly. Best-fit model parameters are obtained where the root mean square (RMS) error of each sample is calculated to be approximately 1 ($r^2 > 0.97$). Table 1 shows the x-dependent volumetric fractions extracted from XPS analyses and calculated from SE data fittings to confirm that the optical model that we develop successfully describes the content of the nc-Si/SiO_x over a wide range of stoichiometries ($0 < x < 2$).

The amount of Si volumetric fraction in "XPS (%)" column is the percentage of all Si-Si bonds, whereas the amount of ($SiO_2 + SiO_x$) shows all Si-O bonds that are extracted from the Si 2*p* signal. The volumetric fractions of Si_2O, SiO, Si_2O_3, and SiO_2 species are

Table 1
The comparison of x-dependent volumetric fractions extracted from XPS peak-fitting analyses and calculated from the SE spectral fittings using the optical model that are developed in this study.

x	XPS (%)		SE (%)		
	Si	$SiO_2 + SiO_x$	SiO_2 + void	Poly-Si	a-Si
0.5	49	52	14	34	40
1.1	5	96	81	9	10
1.2	8	92	84	5	11
1.3	12	87	84	0	16
1.5	0	100	90	0	10
1.7	0	100	100	0	0

extracted separately from the XPS analyses but for the sake of simplicity and to be able to compare with the fittings of SE data we combined them together in the "XPS (%)" column and included it as ($SiO_2 + SiO_x$). Since each SiO_x species in SE calculations cannot be included individually, the amounts of Si_2O, SiO, Si_2O_3, and SiO_2 species are introduced all together as (SiO_2 + void) in the "SE (%)" column. We also add "poly-Si" and "a-Si" components to our SE calculations in order to represent the Si species in the system. As can be seen from Fig. 5, the nanocrystals grow in a vertical direction and the structure resembles to that of porous silicon. This means that a nanocrystal network is surrounded by matrix. In addition, we have determined from XPS analyses that the Si and SiO_2 are not fully phase separated and the matrix is mostly composed of suboxides. Therefore, after a careful optimization of the optical model and the fitting procedure we are convinced that the "poly-Si", used to describe porous silicon and introduced to the model as a combination of "Si + SiO_2 + void" better describes the structure. Given the situation, the "poly-Si" both contributes to "Si" and "SiO_2 + void" columns of XPS analyses. Therefore, poly-Si used in the SE fittings contributes both to Si and (SiO_2 + void) columns of "XPS (%)" in this respect. In summary, the amount of volumetric fractions used in SE spectral data fittings is consistent with the XPS results.

Fig. 6 shows SE spectral data of the ellipsometric angles, Ψ and Δ, and their mathematical fittings calculated using the generic optical model shown in Fig. 5(a) for the three representative regions: Si-rich ($x < 0.9$), SiO_2-rich ($x > 1.7$), and the intermediate ($0.9 < x < 1.3$) regions.

As can be seen from Fig. 6(a) and (c), ellipsometric angles (Ψ, Δ) can be fitted for Si-rich and SiO_2-rich regions with excellent agreement. However, for the intermediate region, there is some deviation from experiment in Fig. 6(b) is not excellent even though its RMS is high ($r^2 = 0.97$). This can be explained by the increased volumetric fractions of substoichiometric species in this region. As mentioned above, we describe the substoichiometric species as a combination of SiO_2 and void in our optical model, where the void fraction is not fully independent, thus preventing an excellent fitting. In addition, there can be stress relaxation in the system when volumetric fractions of the substoichiometric species increase. Barbagiovanni et al. studied Si quantum dots embedded in SiO_2 and performed an extensive XPS analysis, based on which they claim that when Si_2O_3 is present in the system no stress on the quantum dots is observed [13]. Furthermore, through molecular dynamics simulations, Soulairol et al. found that Si_2O helps relieve the stress in Si quantum dots embedded in SiO_2 through a Si—O—Si bridging bonds [14].

In addition, Fig. 6 contains valuable information on the Si crystallization. SE spectra shown in Fig. 6(a) are similar to the well-known SE spectral data of SiO_2, which has oscillatory form. This is to be expected since we know from the XPS analysis (Fig. 4 and Table 1) that when $x > 1.3$ (SiO_2-rich regime) SiO_2 dominates the structure. Moreover, Fig. 6(b) shows a decrease in oscillations and emergence of a broad feature between 4 and 5 eV photon energies, which indicates the formation of nc-Si regions, as confirmed by Fig. 2 and Table 1. The oscillations in Fig. 6(c) are further reduced in the Si-rich regime and the broad feature becomes more prominent between the 3 and 5 eV photon energies. This clearly shows the further crystallization of Si in the system, which is independently confirmed by the TEM and RS analyses (data is not shown here).

Lastly, the real (ε_r) and imaginary (ε_i) parts of the complex dielectric function of the nc-Si/SiO_x thin films for the three representative regions are extracted from the ellipsometric angles (Ψ, Δ) in order to investigate their x-dependencies (Fig. 7). Fig. 7 also indicates the SE spectra of bulk c-Si for the sake of comparison.

As can be seen from the figure, there are prominent oscillations in ε_i and ε_r spectra of the SiO_2-rich region. These oscillations start to decrease for the intermediate and Si-rich regions. In these regions

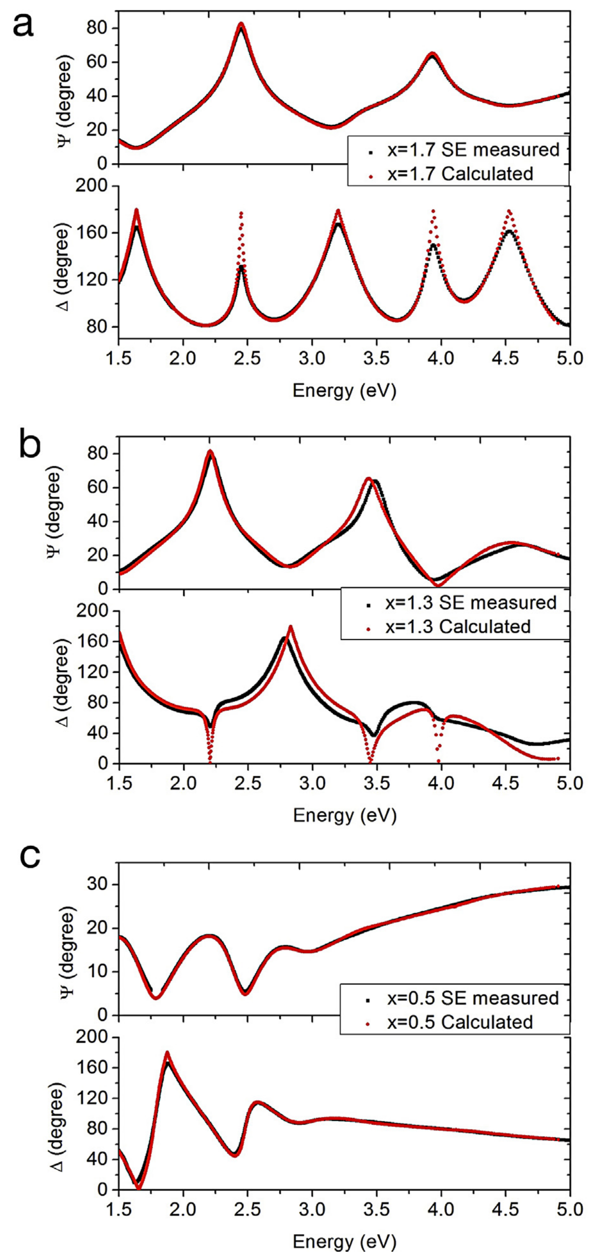

Fig. 6. Graph showing SE spectra of the ellipsometric angles Ψ and Δ and their mathematical fittings calculated using optical model that is developed in this study for (a) SiO_2-rich region (for $x = 1.7$), (b) intermediate region ($x = 1.3$), and (c) Si-rich region ($x = 0.5$).

with the nc-Si formation, two slightly prominent features begin to appear at ~3.3 eV and ~4.3 eV, respectively. These are attributed to the critical points (CP) of c-Si; 3.3 eV for E_1 and 4.3 eV for E_2, respectively. Although the amplitudes of these two points for c-Si spectra are higher and the peaks are narrow, CP of the nanocrystals shows both peak broadening and decreases in amplitude since their finite size distribution broadens the transitions [15]. Due to the crystal sizes being much smaller than the wavelength of laser used, we do not gather primary information (directly from individual nanocrystals), but we do gather secondary information (as a function of the average nanocrystal density) from the nanocrystals. Basically, the presence of the nanocrystals results in minute variations in the effective susceptibility of the medium, which are impressed on the optical phase of the reflected laser beam and in turn are unraveled thanks to the extremely high resolving power of optical

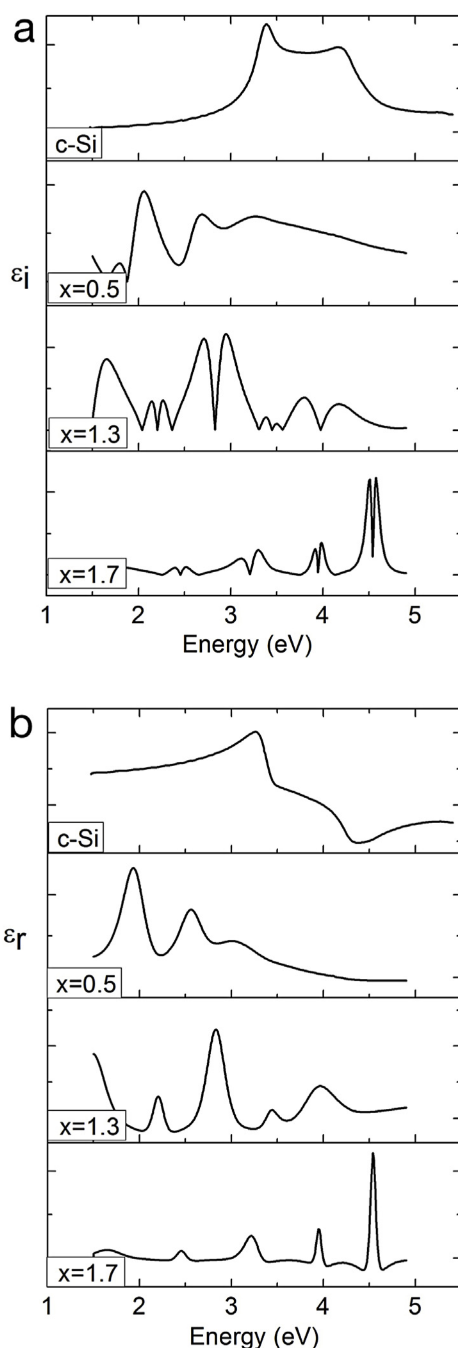

Fig. 7. Graph showing SE spectra of (a) the imaginary part, ε_i, and (b) the real part, ε_r, of the dielectric functions for nc-Si/SiO_x with Si-rich region (x = 0.5), intermediate region (x = 1.3), and SiO_2-rich region (x = 1.7).

phase detection. It is clear from this picture that the strength of any signal from the nanocrystals is proportional to their density. Consequently, we can only observe a slight feature of CP. In their work Kovalev et al. also confirmed this idea [16]. It has been observed in numerous studies that the amplitudes of CP decrease and CP peaks broaden significantly due to small nanocrystal sizes [6,8,16]. One reason may be the negligence of excitonic effects, which are important in bulk spectra [16]. Agocs et al. attributed decrease in the amplitude and the broadening phenomenon to increasing porosity and increasing grain boundaries [6]. Lee et al. made a similar observation and concluded that this can be attributed to the inadequacy of band structure in nanocrystallites due to their extremely small volume and increased surface effects [8].

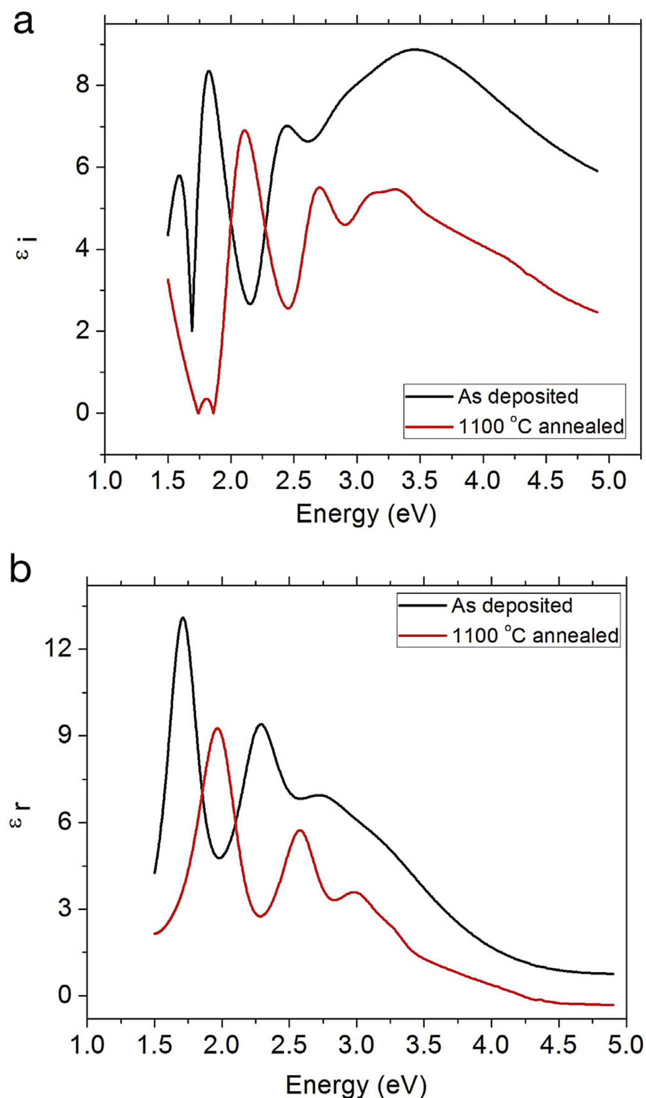

Fig. 8. Graph showing temperature-dependence of (a) imaginary part, ε_i, and (b) real part, ε_r, of the dielectric functions for nc-Si/SiO_x with Si-rich region (x = 0.5).

The sharp intense structures observed for SiO_2-rich region in the dielectric function spectra shown in Fig. 7 suggest a Fabry-Perot-like interference, which point toward a sharp, high-finesse interface between the c-Si substrate and the thin film. This is consistent with our optical model (Fig. 5a) and EFTEM image (Fig. 5b), which shows that the thin film is immediately grown on the c-Si substrate. However, to some extend for the intermediate region, the interference peaks are broadened, which correspond to a low-finesse, rough interface. In addition, for Si-rich region, the interference peaks are further broadened, which correspond to a low-finesse, rough interface between the c-Si substrate and the thin film. This is consistent with the formation of an ultra-thin SiO_2 interface layer between the thin film and the c-Si substrate, which is not very flat. In other words, this SiO_2 interface layer acts in a manner similar to an index-matching layer in the sense of reducing the sharpness of the interface (Fig. 5c). This results in the broadened features observed in Fig. 7. Gravalidis et al. reported a study where they observed growth of the thin films in real time and analyzed optical characteristics of SiO, SiO_x, and SiO_2 [17]. They have also reported dominant interference fringes and related them to multiple reflections of the probe light at the back interface between SiO_x film and c-Si substrate, hence to the thickness and the stoichiometry of SiO_x of the films. Clearly, these features need further study.

We also report on the temperature-dependence of the dielectric functions as shown in Fig. 8(a) and (b). As expected, a significant spectral blueshift is observed when the samples are annealed and Si starts to crystallize. Two prominent features of CP begin to appear at ~3.3 eV and ~4.3 eV, respectively, for ε_i and ~3.1 and ~3.3, respectively, for $\varepsilon_{r.}$

4. Conclusions

In this report, we present a generic optical model to describe the SE spectral data of the nc-Si/SiO_x over an extremely wide range of x values ($0 < x < 2$). In our calculations, we include every possible substoichiometric species for nc-Si/SiO_x and we show that the different combinations of these material systems can be analyzed through the same approach. Relationships between the optical properties and volumetric fractions of the substoichiometric species in these systems are presented. We also show that the optical properties and dielectric functions of the system are highly dependent on the value of x and crystallization.

Acknowledgements

The authors would like to acknowledge Mr. Seçkin Öztürk, Dr. Rene Hübner, and Mr. İlker Yıldız for their efforts in HRTEM, EFTEM, and XPS analyses, respectively. The authors would like to thank Dr. F. Ömer Ilday for useful discussions. This work was supported by the Scientific and Technological Research Council of Turkey (TÜBİTAK) and Federal Ministry of Education and Research Council of Germany (BMBF), 2 + 2 joint project titled "RainbowEnergy" with Grant No. 109R037.

References

[1] L. Pavesi, R. Turan, Si Nanocrystals: Fundamentals, Synthesis, and Applications, Wiley-VCH Verlag GmbH & Co, Weinheim, 2010.
[2] H.G. Tompkins, E.A. Irene, Handbook of Ellipsometry, William Andrew, Inc., NY, 2005.
[3] A. Szekeres, E. Vlaikova, T. Lohner, P. Petrik, G. Huhn, K. Havancsak, I. Lisovskyy, S. Zlobin, I.Z. Indutnyy, P.E. Shepeliavyi, Ellipsometric characterization of SiO_x films with embedded Si nanoparticles, Vacuum 84 (2010) 115–118.
[4] A. En Naciri, M. Mansour, L. Johann, J.J. Grob, C. Eckert, Correlation between silicon nanocrystalline size effect and spectroscopic ellipsometry responses, Thin Solid Films 455–456 (2004) 486–490.
[5] B. Gallas, C.-C. Kao, C. Defranoux, S. Fisson, G. Vuye, J. Rivory, Dielectric function of Si nanocrystals embedded in SiO_2, Thin Solid Films 455–456 (2004) 335–338.
[6] E. Agocs, P. Petrik, S. Milita, L. Vanzetti, S. Gardelis, A.G. Nassiopoulou, G. Pucker, R. Balboni, M. Fried, Optical characterization of nanocrystals in silicon rich oxide superlattices and porous silicon, Thin Solid Films 519 (2011) 3002–3005.
[7] P. Petrik, M. Fried, E. Vazsonyi, T. Lohner, E. Horvath, O. Polgar, P. Basa, I. Barsony, J. Gyulai, Ellipsometric characterization of nanocrystals in porous silicon, Appl. Surf. Sci. 253 (2006) 200–203.
[8] K.-J. Lee, T.-D. Kang, H. Lee, S.H. Hong, S.-H. Choi, T.-Y. Seong, K.J. Kim, D.W. Moon, Optical properties of SiO_2/nanocrystalline Si multilayers studied using spectroscopic ellipsometry, Thin Solid Films 476 (2005) 196–200.
[9] X. Yu, R.J. Zhang, Z.J. Xu, D.X. Zhang, H.B. Zhao, Y.X. Zheng, L.Y. Chen, Optical constants and band gap expansion of size controlled silicon nanocrystals embedded in SiO_2 matrix, J. Non-Cryst. Solids 357 (2011) 3524–3527.
[10] A. En Naciri, M. Mansour, L. Johann, J.J. Grob, C. Eckert, Optical study of Si nanocrystals in Si/SiO_2 layers by spectroscopic ellipsometry, Nucl. Instrum. Methods Phys. Res. B 216 (2004) 167–172.
[11] K. Seino, F. Bechstedt, P. Kroll, Influence of SiO_2 matrix on electronic and optical properties of Si nanocrystals, Nanotechnology 20 (2009) 135702.
[12] J.H. Oh, H.W. Yeom, Y. Hagimoto, K. Ono, M. Oshima, N. Hirashita, M. Nywa, A. Toriumi, A. Kakizaki, Chemical structure of the ultrathin SiO_2/Si(1 0 0) interface: an angle-resolved Si 2p photoemission study, Phys. Rev. B 63 (2001) 205310.
[13] E.G. Barbagiovanni, L.V. Goncharova, P.J. Simpson, Electronic structure study of ion-implanted Si quantum dots in a SiO_2 matrix: analysis of quantum confinement theories, Phys. Rev. B 83 (2011) 035112.
[14] R. Soulairol, F. Cleri, Interface structure of silicon nanocrystals embedded in an amorphous silica matrix, Solid State Sci. 12 (2010) 163–171.
[15] M. Ben-Chorin, B. Averboukh, D. Kovalev, G. Polisski, F. Koch, Influence of quantum confinement on the critical points of the band structure of Si, Phys. Rev. Lett. 77 (1996) 763–766.
[16] D. Kovalev, H. Heckler, G. Polisski, F. Koch, Optical properties of Si nanocrystals, Phys. Status Solidi B 215 (1999) 871–932.
[17] C. Gravalidis, M. Gioti, A. Laskarakis, S. Logothetidis, Real-time monitoring of silicon oxide deposition processes, Surf. Coat. Technol. 180-181 (2004) 655–658.